Pure appl. geophys. 164 (2007) 309–323
0033–4553/07/030309–15
DOI 10.1007/s00024-006-0165-4

Pure and Applied Geophysics

Quantification of Hydrophone Records of the 2004 Sumatra Tsunami

EMILE A. OKAL,[1] JACQUES TALANDIER,[2] and DOMINIQUE REYMOND[3]

Abstract—The 2004 Sumatra-Andaman tsunami was recorded by hydrophones of the International Monitoring System at Site H08 near Diego Garcia, notably in frequency bands extending outside the range of the Shallow Water Approximation. Despite the severe high-pass filtering involved in this instrumentation, we show that the spectral amplitudes recovered around $T = 87$ s can be successfully explained by generation from the seismic source, in the framework of the normal mode theory of tsunami excitation. At the lower frequencies characteristic of more conventional tsunami waves (800 to 3200 s), the signal is probably present in the hydrophone records, but reliable deconvolution of its spectral amplitude is precluded by the fact that the instrumental filters lowered the tsunami signal to the level of resolution of the instrument digitizer. In the context of distant tsunami warning, hydrophone records could provide useful insight into high-frequency tsunami components, and even at lower, more conventional, frequencies, provided that an unfiltered channel could be recorded routinely.

Key words: Tsunami, *T* waves, hydroacoustics, normal mode theory.

Introduction

The catastrophic tsunami generated by the 2004 Sumatra earthquake was recorded not only by traditional tidal gauges (RABINOVICH, 2005), but also by a number of ancillary instruments using a wide variety of technologies, most of which had not been designed for such recording. Actually, some of these techniques had previously detected smaller tsunamis; these include satellite altimetry (SCHARROO *et al.*, 2005), which had identified the 1992 Nicaragua tsunami (OKAL *et al.*, 1999), and the use of GPS receiver arrays to infer variations in the electron content of ionospheric layers affected by the upwards continuation of the tsunami eigenfunction (OCCHIPINTI *et al.*, 2005), as pioneered by ARTRU *et al.* (2005) in the case of the 2001 Peruvian event. Both techniques lend themselves well to the measurement of the

[1] Department of Geological Sciences, Northwestern University, Evanston, IL 60201, USA.
[2] Département Analyse et Surveillance de l'Environnement, Commissariat à l'Energie Atomique, Boîte Postale 12, F-91680, Bruyères-le-Châtel, France.
[3] Laboratoire de Géophysique, Commissariat à l'Energie Atomique, Boîte Postale 640, F-98713 Papeete, Tahiti, French Polynesia.

tsunami on the high seas, unaffected by the complex, site-dependent and often nonlinear process of shoaling and runup which strongly deforms the waves before they can be recorded by tidal gauges.

In the wake of the Indonesian event, LE PICHON *et al.* (2005) also reported for the first time the detection of tsunami-generated signals at infrasound stations of the International Monitoring System (IMS) of the Comprehensive Nuclear-Test Ban Treaty Organization (CTBTO), although the exact mechanism of their generation remains unclear. In addition, YUAN *et al.* (2005), and later HANSON and BOWMAN (2005) reported detections of the arrival of the tsunami wave on horizontal seismometers at several stations on island and continental shores around the Indian Ocean, and suggested that such records may be related to a component of tilt at the relevant stations.

Finally, the 2004 Sumatra tsunami was recorded by hydrophones of the IMS (HANSON and BOWMAN, 2005), notably at Site H08 near Diego Garcia, approximately 2750 km from the epicenter (Fig. 1). These instruments are pressure sensors deployed in the SOFAR channel, at a depth of 1300 m. They are somewhat comparable in concept to the ocean-bottom "tsunameter" sensors of the DART project (TITOV *et al.*, 2005a) in that they capture subtle variations in pressure inside the oceanic water column; however the IMS hydrophones' primary mandate is to detect explosive sources in the ocean, and as such they have been designed as

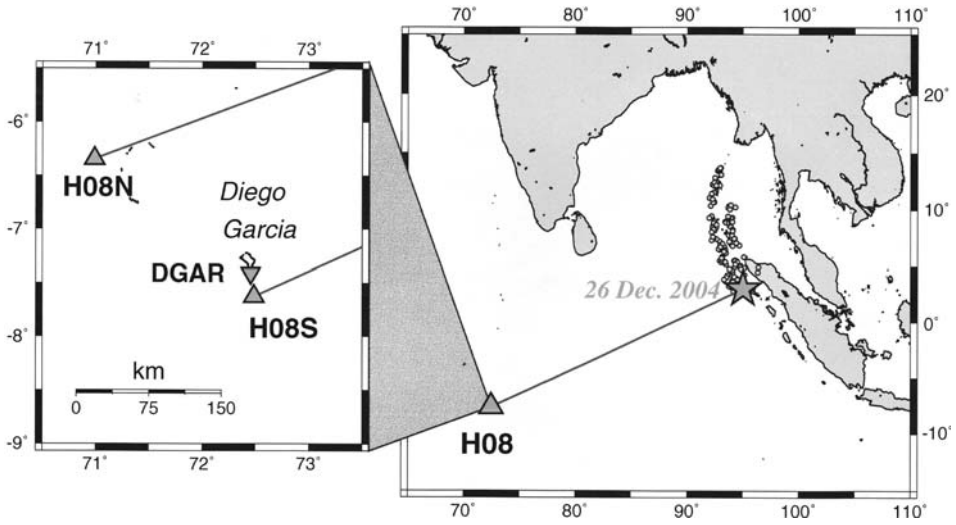

Figure 1
Location of the IMS station H08 at Diego Garcia (triangle), in relation to the 2004 Sumatra earthquake. The star shows the epicentral location of the initiation of rupture, and the smaller symbols the same-day aftershocks, illustrative of the dimension of the fault zone. The inset details the location of the Northern and Southern hydrophone triads, H08N and H08S respectively, relative to the atoll of Diego Garcia, and of the IRIS broadband seismic station (DGAR, inverted triangle), on the atoll itself.

high-frequency instruments, operating at very high sampling rates (250 Hz) and featuring strong high-pass filters in order to eliminate tidal and meteorological sources of noise. Nevertheless, the Sumatra tsunami was so large that it was well recorded even outside the designated frequency band of the instrument.

The purpose of this paper is to analyze quantitatively hydrophone records of the tsunami at Diego Garcia, and to show that order-of-magnitude quantifications of these records can yield acceptable results for the seismic moment M_0 of the parent earthquake in a range of frequencies where far-field tsunamis had not been previously studied, let alone quantified.

The Hydrophone Record at H08S1

As part of the IMS, the hydroacoustic station H08 consists of two triads of instruments tethered to the island of Diego Garcia, BIOT. The Northern group (H08N) is located approximately 200 km to the Northwest of the island, while the Southern group (H08S) is only 25 km due South of the island (Figure 1). In this section, we concentrate on the record from Hydrophone H08S1, part of the Southern triad. The time series under consideration, shown on Figure 2a, starts at 04:00:00 GMT on 26 December, 2004, i.e., 3 hours after the Sumatra event, and runs for 9 hours. It is dominated by acoustic signals, most of which are *T* phases from large and small Sumatra aftershocks. However, as shown on Figure 2b, conventional surface waves are also recorded in the 30-to-100 mHz frequency band from the major aftershocks; the figure also shows energy around 10 mHz, arriving over a window of some 8 hours. This portion of the spectrogram is detailed in Figure 2c which clearly illustrates a strong dispersion. As reported by HANSON and BOWMAN (2005), this is interpreted as the arrival of the tsunami wave, since it matches perfectly the group time predicted by the linear approximation to the Navier-Stokes equations outside the range of validity of the shallow-water approximation (SWA), which predict a dispersion relation between angular frequency ω and wavenumber k of the form

$$\omega^2 = g \cdot k \ \tanh(kH), \tag{1}$$

where g is the Earth's gravity and H the thickness of the water column. The corresponding times, computed for an ocean of depth $H = 4$ km and a source placed at the origin of rupture, as given by the USGS epicentral parameters (3.30°N; 95.98°E; origin time 00:58:53 GMT), are shown as the solid line on Figure 2c.

The spectrogram on Figure 2c documents the presence of substantial amounts of tsunami energy at frequencies significantly higher than for conventional tsunami waves, in particular in the 5 to 13 mHz frequency range. High-frequency tsunami components had been previously described in the gulf of Alaska using early prototypes of tsunameters (GONZÁLEZ and KULIKOV, 1993), and are particularly important to document and study, if possible quantitatively, in view of the

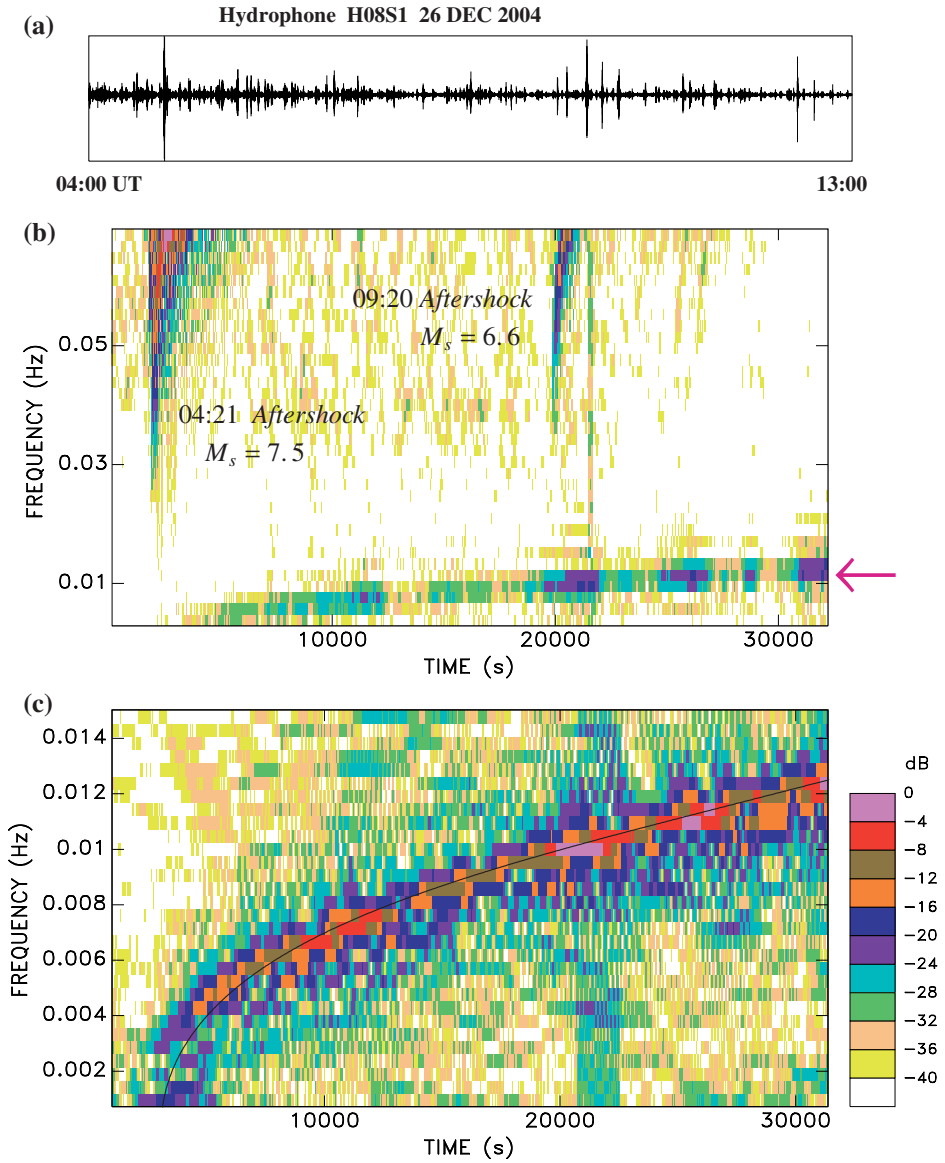

Figure 2

(**a**): Raw time series of the hydrophone record at H08S1, starting 04:00 GMT, i.e., approximately 3 hours after the Sumatra earthquake. (**b**): Spectrogram of the hydrophone record between frequencies of 2.9 and 70 mHz . The diagram is dominated by the Rayleigh waves of two major aftershocks, featuring classic dispersion. The tsunami wave appears as the strongly dispersed branch at $f \leq 0.01$ Hz (red arrow). (**c**): Close-up of the tsunami branch between frequencies of 0.7 and 15 mHz . Note the perfect agreement with the dispersion predicted by (1) (black line). Each pixel is colored according to the palette at right, relative to the maximum spectral amplitude for the spectrogram considered.

observation of anomalous activity in harbors, during which large vessels broke their moorings, up to four hours after the passage of the tsunami waves of reported maximum amplitude (OKAL *et al.*, 2006*a,b,c*). This phenomenon was tentatively interpreted as involving harbor resonances upon the arrival of higher-frequency spectral components of the wavetrain.

In order to quantify the tsunami record at H08S1, it is necessary to first deconvolve the instrument response, outside its designated range of frequencies. As response characteristics are available from the IMS data center only for $f \geq 0.1$ Hz (R. Bowman, pers. comm., 2005), we proceeded to verify the applicability of extending the computation of the response from available poles and zeroes to the frequency range (10 mHz) of the maximum recorded tsunami energy (Fig. 3a). This can be achieved by noting that the hydrophone also recorded conventional Rayleigh waves of the Sumatra earthquake in the same range of frequencies (Fig. 2b). These can be compared directly to the recording at the IRIS seismic station DGAR, on Diego Garcia Atoll, located 25 km from the hydrophone, i.e., considerably less than a wavelength away (Fig. 1). As detailed in the Appendix, a pressure sensor inside the oceanic column will record a long-period Rayleigh wave as an accelerometer whose sensitivity is proportional to the depth of the sensor. Based on this remark, we compare on Figure 3b the spectral amplitudes of the vertical displacements of the

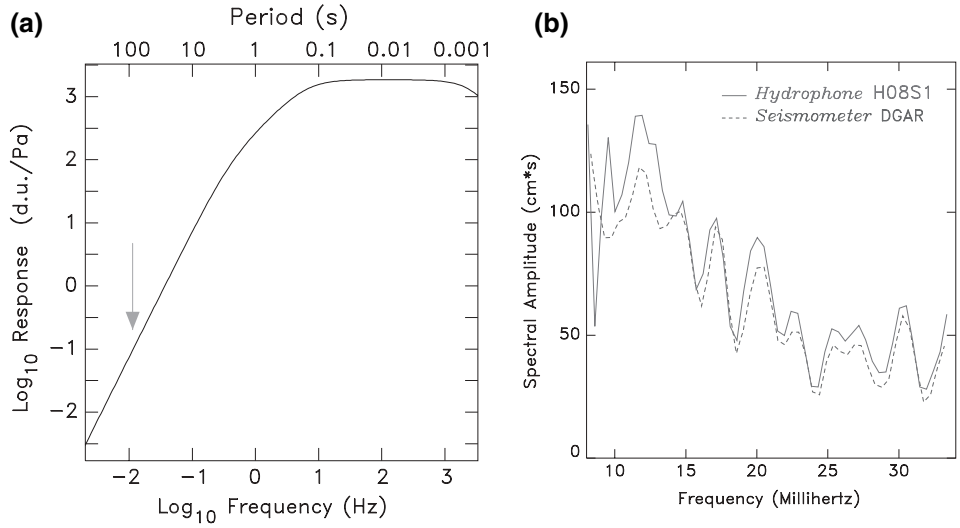

Figure 3

(**a**): Response to pressure of the H08S1 hydrophone, expressed as digital units (d.u.) per Pascal. Note the rapid ω^2 fall-off at low frequencies (e.g., by a factor of 19000 from its nominal value at 100 Hz, for $T = 87$ s; arrow). (**b**): Deconvolved spectra of Rayleigh wave recordings of the Sumatra main shock on the H08S1 hydrophone (solid line) and at the nearby IRIS station DGAR (dashed trace). The former is expressed as equivalent vertical displacement of the ocean floor; see text and appendix for details.

Rayleigh wave trains recorded at H08S1 and DGAR, after appropriate deconvolution of the instrument responses. The agreement between the two spectra is excellent down to 15 mHz, and remains acceptable (within 20%) down to 10 mHz. This means that the calculation of the instrument response using published poles and zeroes can be safely extended to 10 mHz, which is three orders of magnitude or 10 octaves below the cut-off frequency of the main high-pass filters.

With this observation in mind, we elect to quantify the tsunami signal at H08S1 around the local maximum observed at 11.5 mHz ($T = 87$ s), for a group time of 11:17 GMT. We prefer this frequency to the principal signal around 10 mHz at 09:40 GMT, since the instrument response may be less well controlled, and the signal may also be altered by spurious energy in the wake of the large aftershock of 09:20 GMT (Fig. 2*b*). We then isolate a 6000–s window centered on the arrival (note that because of the extreme dispersion, this corresponds to very narrow band-pass filtering, between 81 and 95 s in period), and recover an average spectral amplitude of 2×10^5 Pa*s in this period range, with a peak value of 3.2×10^5 Pa*s (Fig. 4).

We proceed to convert this measurement to that of an equivalent vertical displacement of the ocean surface by computing the eigenfunction of the tsunami at 87 s in the normal mode formalism introduced by WARD (1980). For a 4–km deep ocean, we find that the equivalent normal mode has an orbital number $l = 3450$, a

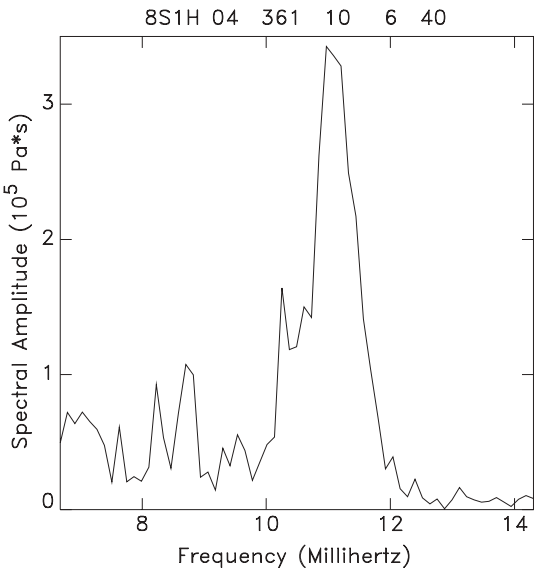

Figure 4
Spectral amplitude of the pressure signal of the tsunami wave deconvolved from the H08S1 trace. The window processed starts at 10:40 GMT and lasts 6000 s. The rapid fall-off of spectral amplitude is due to the extreme dispersion of the branch, under which windowing in the time domain amounts to narrow band-pass filtering.

phase velocity $C = 133$ m/s, and a group velocity $U = 74$ m/s. Figure 5 shows the variation with depth in the ocean column of the vertical displacement and overpressure components of the eigenfunction, respectively y_1 and $-y_2$ in the notation of SAITO (1967) and OKAL (1982) (note that the surface value of y_1 is usually written as η in hydrodynamic applications). The breakdown of the SWA is expressed both by the curvature of these functions (which would otherwise vary linearly with depth), and by the much reduced value of p at the ocean floor (22.2 Pa for $\eta = 1$ cm as opposed to 101 Pa under the SWA). At the sensor depth of 1300 m, we find that the impedance ratio of overpressure to vertical displacement at the surface is 3.95 Pa/cm (solid dot on Fig. 5). Thus, the measured pressure spectral amplitudes convert to spectral amplitudes of equivalent displacement at the surface, $\eta(\omega)$, of 5.1×10^4 cm*s (average) and 8.1×10^4 cm*s (peak value).

In turn, $\eta(\omega)$ is given directly by the classic surface wave excitation formula

$$|\eta(\omega)| = \frac{M_0}{\sqrt{\sin \Delta}} \sqrt{\frac{\pi}{2l}} \frac{a}{U} \left| s_R K_0 - i q_R l K_1 - p_R l^2 K_2 \right| \tag{2}$$

simply adapted from KANAMORI and STEWART (1976) by neglecting anelastic attenuation in the case of tsunamis. For a shallow crustal source, we take $K_0 = 0.12$, $K_1 = 0.5 \times 10^{-5}$ and $K_2 = -0.25 \times 10^{-8}$, in units of 10^{-27}dyn^{-1}. Using a distance $\Delta = 25\,^\circ$, and the initial Harvard CMT focal geometry ($\phi = 329\,^\circ$; $\delta = 8\,^\circ$; $\lambda = 110^\circ$), we find $s_R = p_R = 0.13$; $q_R = 0.92$. The term between vertical bars in (2) is then

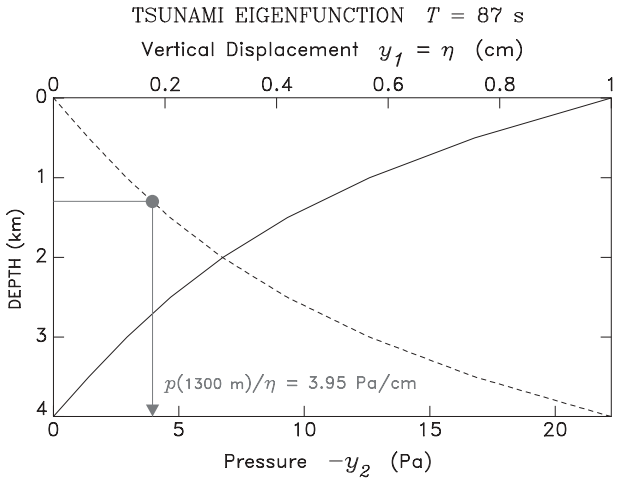

Figure 5
Structure of the eigenfunction of the tsunami in the water column at a period of 87 s. The solid line represents the vertical displacement y_1, normalized to $\eta = 1$ cm at the surface (top scale). The dashed line shows the overpressure $-y_2$ (bottom scale), reaching 22.2 Pa at the ocean floor. The projection of the solid dot (arrow) gives the impedance between the overpressure measured by the hydrophone at a depth of 1300 m and the equivalent wave height on the surface.

2.7×10^{-29}dyn^{-1}. This finally leads to $M_0 = 6.7 \times 10^{29}$ dyn-cm from the average recorded spectral amplitude and $M_0 = 1.1 \times 10^{30}$ dyn-cm from the peak value.

Note that this computation was performed under many drastic approximations, such as the assumption of a homogeneous ocean layer with a constant depth $H = 4$ km, and of a point source double-couple, rather than of the generally accepted model of a 1200–km long rupture (ISHII *et al.*, 2005; GUILBERT *et al.*, 2005; TOLSTOY and BOHNENSTIEHL, 2005). In particular, because of the heterogeneous nature of the distribution of strain release along the fault (e.g., ISHII *et al.*, 2005), it is impractical to attempt to use directivity formulae such as BEN-MENAHEM and ROSENMAN'S (1972), which assume a smooth propagation of the rupture. Note also the jagged nature of the spectrum (Fig. 4), which is reflected in the difference between average and peak spectral values. Under such conditions, the above estimates of M_0 cannot pretend to represent more than an order of magnitude of the size of the seismic source, and the results are, perhaps surprisingly, excellent, as M_0 fits between the initial Harvard CMT solution (3.95×10^{29} dyn-cm), and the larger values later obtained either in the composite Harvard model (1.2×10^{30} dyn-cm; (TSAI *et al.*, 2005)) or by fitting the Earth's gravest normal modes (1.0×10^{30} dyn-cm; (STEIN and OKAL, 2005)).

Hydroacoustic Records of the Main Tsunami Components

In this section, we explore the possibility of detecting, in hydroacoustic records, the main low-frequency components of the tsunami wave, in the period range of their conventional far-field observation (1/2 to 1 hour, or 2000 to 4000 s). We show that a signal is most probably present in the records at H08S1, H08S2 and H08N3, but that the filters applied to the instruments preclude a quantitative interpretation of the recordings.

On Figure 6a, we examine the record of Hydrophone H08N3, part of the Northern triad (Fig. 1), starting 6 hours before the Sumatra earthquake (19:00 UT on 25 December), and lasting 2000 minutes (33.3 hr). After decimation to $\delta t = 1$ s, the record was simply low-pass filtered for $T > 200$ s. Note the distortion of the wavetrain shortly after the predicted arrival of the low-frequency components of the tsunami at 04:37 UT. On the corresponding spectrogram (Fig. 6b), the signal features a maximum of energy around 0.35 mHz at that time. This, and the continuity of the spectrogram along the dispersion curve predicted from (1), warrant the association of this signal with the tsunami. This interpretation is further supported by the agreement between the period of maximum energy (3200 s) and estimates obtained from eyewitness reports in the far field (40 mn to 1 hour) and from the analysis of satellite altimetry data (e.g., OKAL and TITOV, 2007).

Figure 6c presents an attempt to deconvolve the instrument response in the range 0.2–1.25 mHz. This procedure extracts a reasonable signal at the time expected for the tsunami, with a maximum of spectral amplitude at the frequency noted on the

spectrogram (0.35 mHz). However, its interpretation runs into several difficulties. First and foremost, the amplitude of the signal is in excess of 50 kPa peak-to-peak. At such frequencies, the SWA holds, and it predicts an overpressure growing linearly with depth d, $p = \eta\rho_w g d/H$, so that the signal would in turn predict a peak-to-peak wave amplitude on the order of 15 m, which is clearly unacceptable on the high seas, being one order of magnitude greater than measured nearby on the JASON trace (SCHARROO *et al.*, 2005). Note that the latter, being obtained along the track of a fast-moving satellite, constitutes neither a time- nor a space-series (OKAL *et al.*, 1999), and as such does not lend itself to a direct spectral comparison with the hydrophone. The proposed deconvolved amplitude (15 m peak-to-peak) is also one order of magnitude greater than simulated by TITOV *et al.* (2005*b*) in their global numerical model of the propagation of the tsunami on the high seas. Similarly, we cannot envision a meaningful comparison with the tidal gauge record of the tsunami at Diego Garcia (90 cm peak-to-peak), which is not directly interpretable in terms of tsunami height on the high seas, and is sampled at a time step (360 s) sending its Nyquist frequency in the domain of unreliability of the instrumental response of the hydrophones.

In addition, it is clear from the examination of the various frames in Figure 6 that the signal-to-noise characteristics of this putative tsunami signal are weak: Oscillations of nearly comparable amplitude (40 kPa peak-to-peak) and somewhat lower frequency (0.25 mHz) are present both before and after the predicted arrival of the tsunami, the former in the hours preceding the earthquake, their non-causality classifying them irrevocably as noise. On the other hand, similar results are obtained at the hydrophones of the Southern triad, located 220 km away from the Northern group; however, as shown on Figure 7, the maximum spectral amplitude is displaced to 1.25 mHz, and the overpressure amplitudes, while somewhat reduced (to 15 kPa peak-to-peak) remain unacceptably large.

There could be *a priori* several explanations to the unrealistic values obtained when attempting to quantify the relevant spectral amplitudes. They fall in three general categories: (i) signals such as those on Figures 6 and 7 may not be associated with the tsunami; (ii) the hydrophones may be responding to tsunami-induced signals other than the strict overpressure component of the tsunami eigenfunction; and (iii), which we favor, the instrument response used to deconvolve the signal is simply not applicable in the relevant range of frequencies. We reject (i) on the basis of the similarity between the filtered wave shapes at the two groups of hydrophones, as well as the good agreement with the expected arrival times of the tsunami (arrows on Figs. 6 and 7). In addition, the spectrogram shown on Figure 7b is clearly continuous with the higher-frequency one on Figure 2c, the latter lending itself well to quantification. Thus we believe that the signals on Figures 6 and 7 are indeed the principal (low-frequency) components of the tsunami, in the 0.3 to 1.25 mHz frequency range. Regarding (ii), we have assumed that the hydrophone sensors respond to the overpressure $p = -y_2$, neglecting the dynamic pressure $p_{\mathrm{dyn}} = 1/2\rho_w v^2$,

►

Figure 6
(**a**): Hydrophone record at Site H08N3, starting at 19:00 on 25 December 2004, 6 hours before the Sumatra earthquake. The record was simply low-pass filtered for $f \geq 5$ mHz . Note the deformation of the waveform about the time predicted for the tsunami arrival under the SWA (red arrow), the generally noisy character of the record, including before the earthquake, and the very low digit count after filtering. (**b**): Spectrogram of (**a**) between frequencies of 0.1 and 5 mHz. Note the strong energy present at 0.3 mHz at the time of predicted arrival, and the general agreement of the main energy train with the dispersed group times (white line). (**c**): Pressure signal p deconvolved from (**a**) in the frequency band 0.2–1.25 mHz , using available instrument response characteristics. Note the excessive resulting amplitudes.

where v is the particle motion of the water in the wave. Under the SWA, we expect the velocity to be mostly horizontal, $v = \eta C/H$, where C is phase velocity, leading to $p_{\mathrm{dyn}}/p = (1/2)\eta/d$, on the order of 10^{-3} in the present case ($\eta \approx 1$ m; $d = 1300$ m), and thus totally negligible; we have verified from normal mode computations that p_{dyn} is similarly negligible at the higher frequencies featured on Figure 2c.

We are therefore left with hypothesis (iii), namely that it becomes impossible, at the low frequencies involved, to properly deconvolve the instrument response. We note that such frequencies are up to 32000 times lower than the corner frequency of the filter (10 Hz; Fig. 3), and it is unlikely that the published instrumental response remains reliable over 15 octaves. Even if it were, a simple calculation shows that a signal of the amplitude of the JASON trace (1.2 m peak-to-peak) with a period of 3200 s would be reduced to a recorded amplitude of less than 1 digital count. This clearly introduces digitizing noise and makes any quantitative interpretation impossible. We have independently verified that a similar result is obtained when attempting to extract the Earth's free oscillations in the 1–2 mHz range from short-period seismometers: while the gross shape of their spectrum can be recovered, their amplitude becomes unreliable (often times too large) when the instrument response reduces the corresponding signal to a time-domain amplitude of no more than a few digital counts.

Conclusion and Recommendations

The 2004 Sumatra tsunami was recorded by the hydrophones of the IMS at station H08 (Diego Garcia), well outside the frequency range of their designated characteristics. The exceptionally clear dispersion revealed by spectrograms (HANSON and BOWMAN, 2005) is to our knowledge the first documented observation of high-frequency tsunami waves ($f \geq 10$ mHz) in the far field. Our results show that such high-frequency spectral components can be interpreted (within an order of magnitude) in terms of the excitation of the tsunami by the seismic source, in the framework of normal mode theory (WARD, 1980; OKAL, 1988). Thus, the present instrumentation of the IMS hydrophones can provide reliable information regarding the amplitude of such spectral components, which have been documented to pose

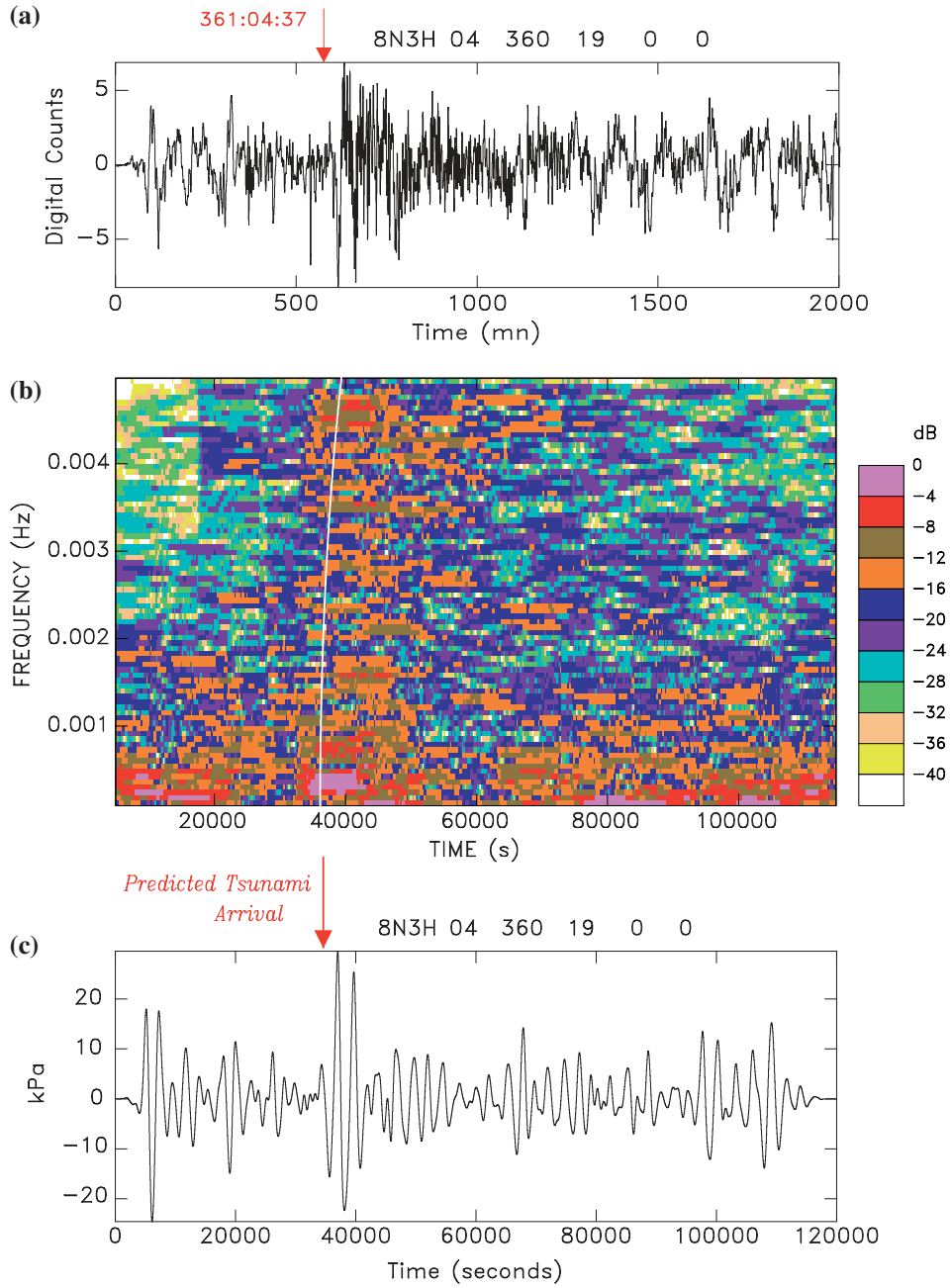

significant hazard in harbors (with the potential for damage to port infrastructures) in the far field (OKAL *et al.*, 2006a,b,c). Because of the strong dispersion involved at those frequencies, such effects can be substantially delayed with respect to tsunami

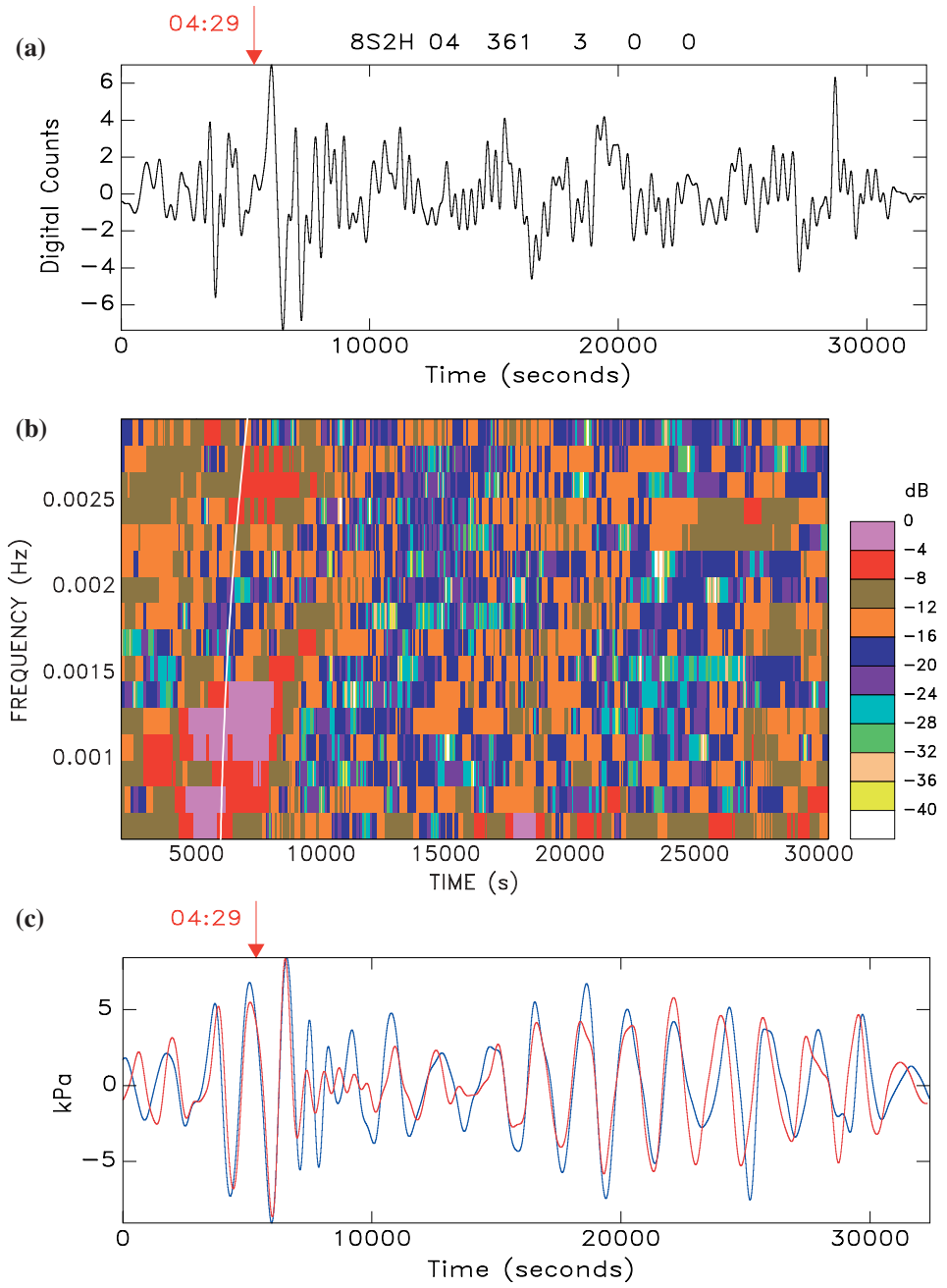

Figure 7

Same as Figure 6 for Hydrophone H08S2 from the Southern triad. The record starts at 03:00 on 26 December, and lasts only 11 hours. The frequency range of the spectrogram (**b**) extends from 0.5 to 3 mHz. On Frame (**c**), records are filtered between 0.5 and 2 mHz , to emphasize the prominent energy present at 1.25 mHz ; the H08S2 record is shown in red, with H08S1 superimposed in blue.

first arrivals, and thus the IMS hydrophones have the potential to contribute significant information for the purpose of transoceanic tsunami warning.

At the lower frequencies ($\approx$ 0.3 mHz) typical of conventional tsunami waves associated with more brutal far-field destruction, we argue that the IMS hydrophones can detect the signal, but that the nature of their present instrumentation (as mandated under the CTBT for the purpose of detecting explosions of much higher frequency content) precludes the deconvolution of a quantitative estimate of the surface amplitude of the tsunami. As the sensors use essentially the same technology as the DART ocean-bottom pressure recorders (TITOV *et al.*, 2005a), this situation evolves entirely from the characteristics of the high-pass filters integrated upstream of recording (in terms of data flow) into the IMS hydrophone systems. We would recommend that, in the future, the original pressure signal be recorded before filtering, so that these instruments could have the possibility of contributing the detection and quantification of a conventional tsunami wave on the high seas, unaffected by shoaling and coastal interaction, to oceanwide tsunami warning algorithms.

Acknowledgments

This research was supported by the National Science Foundation, under Grant CMS-03-01054 and by Commissariat à l'Energie Atomique. We thank Roger Bowman for information on the frequency responses at H08. Several figures were drafted using the GMT software (WESSEL and SMITH, 1991).

Appendix

Response of a Hydrophone to the Passage of a Rayleigh Wave

We consider a Rayleigh wave propagating along the surface of the Earth with a phase factor $\exp i(\omega t - kx)$. Under the shallow water approximation, i.e., if the depth H of the water column satisfies $k \cdot H \ll 1$, we can assume that the dispersion of the Rayleigh wave is unaffected by the ocean. Then, according to Snell's law, the surface wave will be prolonged into the water layer in the form of two progressive waves, one upgoing, the other downgoing, with potentials

$$\phi_1 = A \exp i(\omega t - kx) \exp(-i\gamma z); \qquad \phi_2 = B \exp i(\omega t - kx) \exp(+i\gamma z),$$

where the coordinate z is taken positive upwards and vanishing at the surface of the ocean ($z = -H$ at the bottom), $\gamma^2 = \omega^2/\alpha^2 - k^2$, and α is the velocity of sound in water (1.5 km/s). Boundary conditions impose a zero pressure at the surface ($z = 0$), hence $A + B = 0$, which quickly leads to a vertical displacement field in the water column

$$u_z = -2i\gamma A \cos(\gamma z)$$

and to a pressure

$$p = -\sigma_{zz} = -K\frac{\omega^2}{\alpha^2} A\, 2i \sin \gamma z = -\rho_w \omega^2 2i A \sin(\gamma z),$$

where ρ_w is the density of salt water (1.03 g/cm^3), $K = \rho_w \alpha^2$, and we have omitted the common propagation factor $\exp i(\omega t - kx)$. The ratio of the pressure at depth $-z$ to the vertical displacement at the ocean bottom is thus

$$\frac{p}{u_z|_{z=-H}} = \rho_w \omega^2 \frac{\sin(\gamma z)}{\gamma \cdot \cos(\gamma H)}.$$

In the shallow water approximation ($k \cdot H << 1$ and $\gamma \cdot H << 1$), $\sin(\gamma z) = \gamma z$ and $\cos(\gamma H) = 1$, hence

$$\frac{p}{u_z|_{z=-H}} = \rho_w \omega^2 z \qquad (z < 0).$$

Under these conditions, the hydrophone functions as an accelerometer with a sensitivity proportional to its depth $-z$ in the water layer.

References

Artru, J., Dučić, V., Kanamori, H., Lognonné, P., and Murakami, M. (2005), *Ionospheric detection of gravity waves induced by tsunamis*, Geophys. J. Intl. *160*, 840–848.

Ben-menahem, A. and Rosenman, M. (1972), *Amplitude patterns of tsunami waves from submarine earthquakes*, J. Geophys. Res. *77*, 3097–3128.

Hanson, J.A. and Bowman, J.R. (2005), *Dispersive and reflected tsunami signals from the 2004 Indian Ocean tsunami observed on hydrophones and seismic stations*, Geophys. Res. Letts. *32*(17), L17608, 5 pp.

González, F.I. and Kulikov, Ye. A., *Tsunami dispersion observed in the deep ocean. In Tsunamis in the World* (ed. S. Tinti), pp. 7–16, (Kluwer, 1993).

Guilbert, J., Vergoz, J., Schisselé, A., Roueff, E., and Cansi, Y. (2005), *Use of hydroacoustic and seismic arrays to observe rupture propagation and source extent of the $M_w = 9.0$ Sumatra earthquake*, Geophys. Res. Letts. *32*(15), L15310, 5 pp.

Ishii, M., Shearer, P., Houston, H., and Vidale, J. (2005), *Rupture extent, duration and speed of the 2004 Sumatra-Andaman earthquake image by the Hi-Net array*, Nature *435*, 933–936.

Kanamori, H. and Stewart, G.S. (1976), *Mode of the strain release along the Gibbs fracture zone, Mid-Atlantic Ridge*, Phys. Earth Planet Inter. *11*, 312–332.

Le Pichon, A., Herry, P., Mialle, P., Vergoz, J., Brachet, N., Garcés, M., Drob, D., and Ceranna, L. (2005), *Infrasound associated with 2004–2005 large Sumatra earthquakes and tsunami*, Geophys. Res. Letts. *32*(19), L19802, 5 pp.

Occhipinti, G., Lognonné, P., Kherami, A., and Hébert, H. (2005), *Modelling and detection of the ionospheric perturbation associated with the Sumatra tsunami of December 26th, 2004*, Eos, Trans. Amer. Geophys. Un. *86*(52), U11A–0829, [abstract].

Okal, E.A. (1982), *Mode-wave equivalence and other asymptotic problems in tsunami theory*, Phys. Earth Planet. Inter. *30*, 1–11.

Okal, E.A. (1988), *Seismic parameters controlling far-field tsunami amplitudes: A review*, Natural Hazards *1*, 67–96.

OKAL, E.A. and TITOV V.V. (2007), M_{TSU}: *Recovering seismic moments from tsunameter records*, Pure Appl. Geophys. *164*, 309–323.

OKAL, E.A., PIATANESI, A., and HEINRICH, P. (1999), *Tsunami detection by satellite altimetry*, J. Geophys. Res. *104*, 599–615.

OKAL, E.A., FRITZ, H.M., RAVELOSON, R., JOELSON, G., PANČOŠKOVÁ P., and RAMBOLAMANANA, G. (2006*a*), *Field survey of the 2004 Indonesian tsunami in Madagascar*, Earthquake Spectra, *22*, S263–S283.

OKAL, E.A., FRITZ, H.M., RAAD, P.E., SYNOLAKIS, C.E., AL-SHIJBI, Y., and AL-SAIFI, M., (2006b), *Field survey of the 2004 Indonesian tsunami in Oman*, Earthquake Spectra, *22*, S203–S218.

OKAL, E.A., SLADEN, A., and OKAL, E.A.-S. (2006c), *Field survey of the 2004 Indonesian tsunami on Rodrigues, Mauritius and Réunion Islands*, Earthquake Spectra, *22*, S241–S261.

RABINOVICH, A.B. (2005), *The Great Sumatra tsunami of December 26, 2004: Observation and analysis*, Geophys. Res. Abstr. *7*, 05-A-11061, [abstract].

SAITO, M. (1967), *Excitation of free oscillations and surface waves by a point source in a vertically heterogeneous Earth*, J. Geophys. Res. *72*, 3689–3699.

SCHARROO, R., SMITH, W.H.F., TITOV, V.V., and ARCAS, D. (2005), *Observing the Indian Ocean tsunami with satellite altimetry*, Geophys. Res. Abstr. *7*, 230, [abstract].

STEIN, S. and OKAL, E.A. (2005), *Size and speed of the Sumatra earthquake*, Nature *434*, 581–582.

TITOV, V.V., GONZÁLEZ, F.I., BERNARD, E.N., EBLE, M.C., MOFJELD, H.O., NEWMAN, J.C., and VENTURATO, A.J. (2005*a*), *Real-time tsunami forecasting: Challenges and solutions*, Natural Hazards *35*, 41–58.

TITOV, V.V., RABINOVICH, A.B., MOFJELD, H.O., THOMSON, R.E., and GONZÁLEZ, F.I. (2005b), *The global reach of the 26 December 2004 Sumatra tsunami*, Science *309*, 2045–2048.

TOLSTOY, M. and BOHNENSTIEHL, D.R. (2005), *Hydroacoustic constraints on the rupture duration, length and speed of the great Sumatra-Andaman earthquake*, Seismol. Res. Letts. *76*, 419–425.

TSAI, V.C., NETTLES, M., EKSTRÖM, G., and DZIEWOŃSKI, A.M. (2005), *Multiple CMT source analysis of the 2004 Sumatra earthquake*, Geophys. Res. Letts. *32*(17), L17304, 4 pp.

WARD, S.N. (1980), *Relationships of tsunami generation and an earthquake source*, J. Phys. Earth *28*, 441–474.

WESSEL, P. and SMITH, W.H.F. (1991), *Free software helps map and display data*, Eos, Trans. Amer. Geophys. Un. *72*, 441 and 445–446.

YUAN, X., KIND, R., and PEDERSEN, H.A. (2005), *Seismic monitoring of the Indian Ocean tsunami*, Geophys. Res. Lett. *32*(15), L15308, 4 pp.

(Received May 6, 2006, accepted June 15, 2006)